LLNL-JRNL-865947

How Rains and Floods Become Groundwater: Understanding Recharge Pathways With Stable and Cosmogenic Isotopes

J. Lerback, A. Visser, A. J. Harm, E. Oerter, R. Bibby, J. Danielsen, K. Minn, M. Garguilo, E. Grande

June 24, 2024

Hydrological Processes

How Rains and Floods Become Groundwater: Understanding Recharge Pathways with Stable and Cosmogenic Isotopes

AUTHORS

Jory Lerback[1], Richard Bibby[1], Jacob Danielsen[2], Mike Garguilo[2], Emilio Grande[3], A. Jake Harm[1,3], Ken Minn[2], Jean Moran[3], Erik Oerter[1], and Ate Visser[1]

[1] Lawrence Livermore National Laboratory, Division of Nuclear and Chemical Sciences
[2] Zone 7 Water Agency, Division of Water Resources
[3] California State University, East Bay, Department of Earth and Environmental Sciences

Corresponding Author: lerback1@llnl.gov

ABSTRACT

Anthropogenic climate change leads to increased precipitation intensity and exacerbated droughts in California, challenging the reliability and drought resiliency of water supply. Storing floodwater underground via managed aquifer recharge can mitigate these effects through direct infiltration or streambed infiltration. Seasonally dry streams (arroyos) already play an important part in managing groundwater recharge to the Livermore basin (CA). Understanding how, when, and where stormwater and arroyo water infiltrate is critical to effectively utilize this strategy. To track water from recent storms (water year 2022-2023, WY23) into the Livermore Valley Groundwater Basin, we analyzed stable water isotopes ($\delta^{18}O$ and δ2H) in combination with naturally occurring radioactive isotopic tracers, sulfur-35 (^{35}S, t½=87 days) and tritium (^{3}H, t½=12.3 years).

By comparing measurements of $\delta^{18}O$, ^{35}S, and ^{3}H in arroyos to precipitation and groundwater, we classified the relative age and identified source of recharge to 16 wells near two arroyos. Two wells contained water with recent recharge (from WY23) from local precipitation. One well had recent recharge from variable (precipitation and imported water) sources. One well contained imported water recharge. Three wells contained water from mixed recent and older (pre-WY23) waters, from local precipitation sources. Two wells contained recent recharge from local mine settling ponds. Seven wells had older recharge from local precipitation sources.

This combination of isotopes allows us to delineate where local and imported water recharges in this highly managed basin and identify locations where managed aquifer recharge is contributing to rapid groundwater infiltration. Our combined interpretation of isotopic water ages and sources in the context of land use shows that local infiltration of precipitation in open spaces is an important recharge mechanism, in addition to the managed arroyo recharge. A broader familiarity with ^{35}S will enable more extensive research on the infiltration of urban floodwaters.

Keywords: isotopes, groundwater, hydrology, managed aquifer recharge, sustainable management, sulfur-35, oxygen-18, tritium

1. INTRODUCTION

Anthropogenic climate change is bringing changes to the water cycle, resulting in earlier-in-the-season snowmelt and warm coastal storms that will flood and damage aging water storage infrastructure (Kuang et al., 2024; Kundzewicz & Döll, 2009; Siirila-Woodburn et al., 2021). Flood, drought, and contamination risk from the intensified water cycle will harm already economically and socio-culturally disenfranchised communities. To ensure long-term groundwater sustainability despite climate change driven hydrologic conditions, the State of California (CA) in the United States of America enacted the Sustainable Groundwater Management Act (SGMA) in 2014. SGMA requires the development of Groundwater Sustainability Plans (GSPs) to address six sustainability criteria, including aquifer depletion that threatens water supplies and groundwater-dependent ecosystems. Managed aquifer recharge (MAR), and in particular flood-MAR, has been proposed as a tool to mitigate excess water (from storms and flooding), as well as aquifer depletion (from drought and pumping demands) (Marr et al., 2018). MAR encompasses any intentional recharge of water to aquifers for subsequent recovery or environmental benefit (Council, 2009).

MAR has been practiced for millennia through spreading water and other land management practices, and in the past several decades, intentional MAR (and associated technical research) has accelerated to meet the increasing demand for groundwater resources (Dillon, 2005; Dillon et al., 2018; Joël Casanova; Zhang et al., 2020) As of 2021, nearly 200 new MAR projects have been proposed in CA in groundwater sustainability plans. Most of these projects involve spreading water in basins or agricultural lands and only ten involve channel infiltration projects (Ulibarri et al., 2021). The International Groundwater Resources Assessment Centre (IGRAC, 2016) estimated that river water was the most commonly (approximately 50%) characterized source water for MAR projects, with stormwater the second most common (approximately 20%). This study focuses on MAR of stormwaters through existing ephemeral stream channels and associated floodplains.

Several approaches are commonly applied to estimate the efficiency of MAR operations, both in the planning stages and during operation. Numerical models support the technical development of MAR plans through the simulation of flow and solute transport to evaluate sustainability and hazards in MAR systems (Ringleb et al., 2016). Hydrograph analyses for water table fluctuations have given estimates of recharge and connectivity to surface water systems (Águila et al., 2019); however, heterogeneity in aquifer materials and proper attribution of water table fluctuation drivers (e.g., flood event versus pumping) generates uncertainties, where groundwater pumping is especially influential in agricultural and urban water systems.

Analyzing naturally-occurring isotopic tracers can help identify the spatial heterogeneity of infiltration and quantify the importance of distinct water sources to aquifer recharge (i.e. local precipitation or imported stream water) (Klaus & McDonnell, 2013; Tetzlaff et al., 2014; Visser et al., 2018). Water stable isotopes (oxygen and hydrogen, hereafter $\delta^{18}O$ and $\delta^{2}H$) are commonly used to build mixing models (Kirchner, 2019; Marx et al., 2021). Multiple isotope systems provide better constraints when isotopic endmember signatures are not stable in time due to radioactive decay, natural variability in the source waters, or operational water management. The addition of radioactive, cosmogenic tracer systems such as sulfur-35 (^{35}S, $t_{½}$=87 days) and tritium (^{3}H, $t_{½}$=12.3 years) allows for examining the timescale of flow paths. ^{35}S is an indicator of the newest water fraction (e.g., “same year”, “young water” or “recent recharge”) because radioactive decay reduces its concentration to 5% in one year (Urióstegui et al., 2017). ^{3}H concentrations reflect residence times on decadal timescales and can indicate mixing with pre-modern water that recharged before nuclear testing started in the 1950s (Tolstikhin & Kamenski, 1969).

Multi-source waters complicate the interpretation and understanding of MAR operations. For channel or in-stream recharge, three potential sources of water recharge (local precipitation, natural arroyo flows, and imported water) commonly cannot be separated using a single isotopic tracer in highly managed aquifers. We applied three ($\delta^{18}O$, ^{3}H, and ^{35}S) tracer systems to address the following research questions: Does new, local water infiltrate the upper aquifer such that it can be detected in nearby, shallow monitoring wells? Does groundwater recharge occur homogeneously along the arroyo channels and associated floodplains?

Overall, this paper investigates how naturally-occurring and short-lived isotope systems are useful in disentangling the source waters recharging mixed natural and engineered water systems. The combination of $\delta^{18}O$, $\delta^{2}H$, ^{3}H, and ^{35}S leading to this new understanding of recent, local floodwater tracking will provide water managers with the scientific basis to optimize and verify MAR projects for sustainable water management planning under dynamic hydroclimates and increasing water demands.

2. METHODS

2.1 Site Description

The study site in Livermore Valley and the connected Amador Valley comprises an east-west trending valley (Livermore Amador Valley hereafter) in the Central CA Coast range, located in Alameda County approximately 60 km east of San Fransico (Figure 1A). The site includes the urban areas of Livermore and Pleasanton, agricultural areas (primarily vineyards), and encompasses the surrounding hills that are reserved for open space.

Intermittently dry streams (locally and herein termed "arroyos") are a major hydrologic feature and are important for groundwater recharge sustainability planning. Recharge timing and volumes are currently modelled with a surface water budget—differences in stream gage flows are attributed to groundwater recharge (negative difference downstream) or groundwater discharge (positive difference downstream) (Zone 7, 2023); however, this method does not capture heterogeneity of infiltration potential, the overall volume recharging the aquifer (as opposed to being used by groundwater dependent ecosystems), nor over-bank flooding (bypassing stream gages).

Livermore Amador Valley is located in the Central CA Diablo Range, bounded to the west by Pleasanton Ridge and the Calaveras Fault Zone, to the east by the Greenville Fault,(Hartzell et al., 2016) and to the north by Mount Diablo. To the south, surface exposures in the Range consist of Plio-Pleistocene nonmarine rocks (Hartzell et al., 2016). The valley has a topographic slope towards the west (Carpenter et al., 1984). Valley fill is Quaternary alluvium from a depth of approximately 30 m on the eastern edge of the Valley, to over 200 m on the western edge. These sediments are underlain by the Livermore Formation, consisting of Plio-Pleistocene sandy gravel interbedded with clay lenses serving as aquitards (Figure 1B) (Moore et al., 2006; Moran et al., 2002).

The lithology includes an upper aquifer of alluvial sand and gravel, over a lacustrine clay aquitard. The wells sampled in this study primarily target the upper alluvial aquifer unit to understand the most recent recharge nearest the surface recharge areas (Figure S1). The lower aquifer unit underneath the aquitard comprises of the Upper and Lower Livermore Formation. These Livermore Formations are sand and gravel, based on the well log lithologies provided in the Supplementary Information. The central and western region of the Livermore Amador Valley Main Basin has a clay overburden which impacts three sampled wells (20C7&8, 10N2&3, and 16P5; locations in Figure 1B and Figure S1).

The study site has a semi-arid Mediterranean climate and a mean annual temperature of 15.6°C (1991-2020). Annual precipitation is approximately 45 cm, of which 90% falls between November and April (Moore et al., 2006; PRISM, 2014) (Figure 2A). Total estimated annual reference evapotranspiration for this area (California Irrigation Management Information System station 191) is approximately 130 cm in 2023 (CIMIS, 2024). Livermore Amador Valley experienced two multi-year severe droughts in the previous decade, followed by an exceptionally wet water year, water year 2023 (WY23, this study period) with over 60 cm of rain (Akyuz, 2017; Zone 7, 2023).

We studied recharge from two arroyos: Arroyo Mocho and Arroyo Valle (hereafter referred to as "AM" and "AV"). The arroyos start in the hills south of the Livermore Amador Valley flowing north and west through the cities of Livermore and Pleasanton, eventually exiting the basin through Arroyo de la Laguna to the southwest, and ultimately flowing into the San Francisco Bay through Alameda Creek (Figure 1). Natural flows typically stop in April, with the cessation of the local rainy season, causing the arroyos to go dry.

The naturally gravelly streambeds allow the arroyos to be used as recharge zones by the local water agency, 'Zone 7' (Zone 7, 2023). Zone 7 has rights to divert water imported from the

Sacramento-San Joaquin River Delta via the South Bay Aqueduct (SBA) (Figure 1B). The SBA waters are released directly into arroyo stream channels or piped into Reservoir Del Valle. As a result, Reservoir Del Valle is a mixture of local precipitation (including natural inflow to the reservoir) and water stored from the SBA, which is connected to the northern end of the reservoir. In addition to arroyo recharge, active quarry operations in the Livermore Amador Valley have resulted in a complex and dynamic series of reclaimed and actively mined pits called the Chain of Lakes (Figure 1A). The western-most lakes are old gravel quarries where operations are completed and are now lakes used for storage and in connection with underlying aquifers and are therefore used for groundwater recharge. Silt ponds and de-watering operations associated with the active quarries are clay-lined and are not believed to be hydraulically connected to the underlying aquifers.

We estimated the source water composition of AM and AV based on three stream gages (AVNL, AMNL, and AMHAG), Del Valle Reservoir releases, and diversion rates from SBA (Zone 7, 2023). We distinguish between flows, imported water, and flood waters. Natural flows into AM are measured at the AMNL gage (Figure 1B) because it is not impacted by SBA or reservoir releases at this location. Natural flow in AV is calculated from the ANVL gage while accounting for (removing the contribution from) reservoir and SBA releases. Increases in streamflow below the gages AVNL and AMNL are considered flood waters, where lower-elevation runoff flows over stream banks into the stream channels (Figure 1B).

The Livermore Valley Alternative Groundwater Sustainability Plan (Alt-GSP) includes a water budget which accounts for recharging groundwater via the arroyos. This recharge is calculated by taking the difference between flow into (measured flows at AMNL and AVNL plus imported water) and out of the arroyos at the end of areas of known recharge (Figure 1B). These models represent maximum recharge values and do not account for evapotranspiration nor overbank flooding. Applied water in the groundwater recharge models is an estimate of excess urban and agricultural irrigation reinfiltrating to the aquifer.

Annually, an average of 5.7 million m^3 per year of groundwater is pumped out of the basin aquifer for municipal, agricultural, and industrial use. Zone 7 Water Agency estimates an average of 12 million m^3 per year was recharged through AM and AV in 2012-2022, and 27 million m^3 in WY23.

2.2 Research Design

The arroyos in the Livermore Amador Valley are underlain by coarse sediments that act as losing streams and are effective for groundwater recharge into the Livermore Valley Groundwater basin (Zone 7, 2023). In addition, because WY23 was a particularly wet year with water inundation throughout the arroyo floodplains, we expected to find arroyo water recharging to nearby wells, in addition to infiltration of local rain to the upper aquifer.

The models that support the Livermore Valley Groundwater Basin Alt-GSP calculate the total volume of recharge across entire reaches of the gaged arroyo but do not account for heterogeneity within reaches. We expect more infiltration will occur in the upstream portions of the arroyos, where there is open space and agriculture, and where the natural arroyo channels are composed of gravel. In contrast, we expect the downstream portions of the arroyos will have relatively less infiltration as the arroyos are underlain with clays or concrete-lined engineered channels in urban areas and surrounded by paved surfaces. We therefore used isotope geochemistry to investigate the spatial variation in recharge mechanisms, in terms of the distance of the wells from the recharge sources and the land use surrounding the sampled wells.

2.2.1 Isotopes as Hydrological Tracers

$\delta^{18}O$ and $\delta^{2}H$, colloquially referred to as "water stable isotopes", have been applied in urban hydrology to distinguish water sources (e.g. groundwater or surface waters) and seasonality (Jameel et al., 2018; Marx et al., 2021; Visser et al., 2018). While stable water isotopes have been used to understand the seasonal origin of a given water sample, this requires a distinct seasonal signal in the surface waters which is not available in semi-arid regions with highly variable input signatures and further complicated by engineered systems importing water from multiple locations (Mamand & Mawlood, 2023; Xia et al., 2023; Ye et al., 2022).

^{35}S is a naturally occurring short-lived radioisotope with a half-life of 87 days (Brothers et al., 2010). Cosmogenic ^{35}S, produced from the spallation of argon-40 in the upper atmosphere by cosmic rays, is oxidized to $^{35}SO_4^{2-}$ (Schubert et al., 2020). The ^{35}S isotope system is a recently developed tracer for groundwater, and has been applied to understand hydrology in high elevation, mountainous watersheds with little human impact (Deinhart et al., 2021; Michel & Natfz, 1995; Priyadarshi et al., 2014; Shanley et al., 2005; Urióstegui et al., 2017; Visser et al., 2019). Method development studies have been applied in low-elevation, human-impacted (urban) MAR systems, but these studies have not yet used ^{35}S to characterize mixing between multiple sources or recharge waters (Clark et al., 2016; Uriostegui et al., 2015). Other studies have shown the variation in ^{35}S in precipitation as having some utility as scaled with other cosmogenic isotope tracers such as beryllium-7 and tritium (^{3}H) (Schubert et al., 2020; Schubert et al., 2021; Yoon et al., 2023).

^{3}H is a naturally-occurring radioisotope of hydrogen that is produced by cosmic radiation in the upper atmosphere (Poluianov et al., 2020). Anthropogenic sources of tritium include nuclear power reactors and research facilities. Legacy tritium from above-ground nuclear testing still resides in the oceans and in groundwater that recharged between 1950 and 1990 (Clark & Fritz, 1997). With a half-life of 12.3 years, it has been applied as a natural tracer for calculating groundwater age and distinguishing between modern groundwater (recharged after 1950) and pre-modern groundwater (recharged before 1950) (Carlson et al., 2011; Di Renzo et al., 2023; Lindsey et al.; Telloli et al., 2022; Visser et al., 2016).

2.2.2 Isotope Sample Collection

Water samples were collected from regionally representative precipitation, surface waters, and groundwater wells. Groundwater samples were analyzed to identify which one of three potential sources contributed to recharge: (1) infiltration of local precipitation, (2) infiltration of arroyo waters during natural flows (e.g. winter flooding), and (3) infiltration of arroyo waters during the diversion of imported water into the arroyos. To make the distinction between these three endmembers, the isotopic signature of each potential recharge water source was analyzed throughout WY23.

Precipitation was collected daily for δ^2H and $\delta^{18}O$ analyses since 2017 at the same location, with ~10 km of the study sites (n = 176, n_{WY23} = 47). Monthly integrated samples for tritium analyses were collected between December 2022 and March 2023 (n=6). Three ^{35}S precipitation samples were collected in Oakland (CA), 64 km west of Livermore, as part of a separate study.

Surface waters were sampled for δ^2H and $\delta^{18}O$ analyses (n = 36), tritium (n = 26), and ^{35}S (n = 26) to understand the temporal variability of isotopic signatures in the potential surface water inputs to the Livermore aquifer system. AM was sampled repeatedly at Concannon Road (Figure 1). Additional samples were collected higher up in the watershed, just below the SBA culvert, and further downstream in an area with surface water – groundwater exchange (Figure 1). AV was repeatedly sampled at Sycamore Grove and additional samples were collected from Reservoir Del Valle, upstream of the Livermore basin (Figure 1).

We sampled 25 groundwater wells at variable distances from both arroyo systems. The midpoint depth of the screened interval ranged from 3.5 to 93 m with an average depth of 27.1 m. 17 wells were screened in the upper aquifer and 8 nested wells were sampled to identify potential connectivity between the upper and lower, confined aquifer. Wells were sampled for δ^2H and $\delta^{18}O$ (n = 34, with 8 resampled wells, 25 distinct wells), ^3H (n = 5), and ^{35}S (n = 23, with 6 resampled wells, 16 distinct wells) by the authors and by Blaine Tech Services (San Jose) in summer and fall 2023. Wells were purged until the specific conductance and pH measured by a multiparameter probe (ThermoProbe, Inc., Pearl, USA) were stable for at least 10 minutes prior to sample collection.

2.3 Procedures for Field Collection and Laboratory Analyses

Water samples for δ^2H and $\delta^{18}O$ analyses were collected in dry 20 mL glass vials with polyseal cone caps to prevent evaporation. Liquid water samples were analyzed using a cavity ring down spectroscopy instrument (L-2140i; Piccarro, Inc., Santa Clara, CA, USA). Stable isotope values are reported using δ notation, where $\delta = (R_{sample}/R_{standard}) - 1$. In this notation, R_{sample} and $R_{standard}$ are the $^2H/^1H$ or $^{18}O/^{16}O$ ratios for the sample and standard, respectively, and referenced to the Vienna standard mean ocean water standard (Coplen, 1995). The standard deviation of repeated analyses of calibration standards run for each sample set ranged from 0.07 to 0.16‰ for $\delta^{18}O$, and 0.15 to 0.46‰ for δ^2H, which we take to represent the uncertainty of $\delta^{18}O$ and δ^2H measurements herein.

^{35}S samples were collected in clean 20 L High-Density Polyethylene (HDPE) containers that were triple-rinsed with sample water before collection. Samples were analyzed following procedures and error propagation described in (Deinhart et al., 2021). Sulfate content was on average 20 mg/L for groundwaters and 35 mg/L for surface waters. For precipitation samples with very low sulfate concentration, a sodium sulfate carrier was added. Briefly, sulfate was concentrated using 20 g Amberlite anion exchange resin, eluted with 150 mL sodium chloride, and organics were cleaned with 10 mL of 10% nitric acid and 3 mL of 30% hydrogen peroxide. Sulfate was then precipitated as barium sulfate by addition of barium chloride, decanted of acid, rinsed with deionized water and dried. The sulfate was then suspended in an Instagel Plus liquid scintillator cocktail. Samples were analyzed via low level beta decay counting in a 1220 QUANTULUS Ultra Low Level Liquid Scintillation Spectrometer (PerkinElmer, Shelton, U.S.A.). The analytical error (2σ) ranged from 0.09 to 0.37 mBq/L and represents the nuclear counting error. Typically, because it exceeds 20% of the activity value, propagating the smaller source of errors is not a significant contributor to the overall error budget in light of the low count rates (Currie, 1968). The Minimum Detectable Activity (MDA) ranged from 0.11 to 0.40 mBq/L with a mean of 0.31 mBq/L (SD = 0.07 mBq/L, n = 49). Duplicate samples were collected to constrain uncertainty and are discussed in the Supplemental Information. Because of the 87-day half-life of ^{35}S, the activity concentrations were decay-corrected to 1 July 2023 and 1 October 2023, to directly compare surface and ground water activities.

Tritium samples were collected in 1L clean HDPE bottles and analyzed by helium-3 in-growth (Clarke et al., 1976; Surano et al., 1992). 500 mL was loaded into a stainless steel container. The atmospheric gases, including helium-3, were removed from the sample with a turbomolecular pump. The samples were stored under vacuum for a minimum of three weeks to accumulate helium-3 from tritium decay. Helium-3 was measured on a VG5400 sector field mass spectrometer system with an automated sample processing manifold. The instrument detection limit was 1 pCi/L.

3. RESULTS

3.1 Arroyo Flows and Composition

Water diversions from the SBA in WY23 amounted to 9.4 million m^3 (7.7 TAF) whereas average imports were 8.4 million m^3 (6.9 TAF) per year in the preceding decade (WY12-13 to WY21-22). In comparison, less than 2 million m^3 (1.6 TAF) were imported in each of the two years leading up to our study due to the drought.

Storms in mid-winter (late December and January) and early spring (April) during WY23 led to two episodes of high flows in both arroyos (Figure 3). AM recorded flows of up to 1.4 million m^3/day (or 1.1 TAF/day) on December 31, 2022. AV recorded flows of 5.1 million m^3/day (or 4.2 TAF/day) on January 13, 2023. In the winter and spring months, the major contributors to stream flow were natural flows (characterized as runoff from the hills and within the valley that enter the arroyo channels) and flood water releases (water released into Arroyo Valle from the Lake Del Valle Reservoir to alleviate reservoir flooding), with a notable mid-winter reservoir release in AV. The imported water from the SBA was released intermittently in the winter when there were very low flows in the arroyos and increased as a percent of stream flow through the spring, reaching nearly 100% of stream water in June in AM and July in AV.

Based on the composition of water in the arroyos, we distinguish three periods of recharge in WY23 for further isotopic analysis: 1) before the summer release of imported water (January-June, time period 1), 2) during the summer release of imported water (July-August, time period 2), and 3) after the release of imported water (September-October, time period 3).

3.2 $\delta^{18}O$ in Source Waters and Groundwater

Stable water isotope signatures ($\delta^{18}O$ and $\delta^{2}H$) were analyzed to understand differences and temporal variability in groundwater recharge sources. We describe here the $\delta^{18}O$ data, while $\delta^{2}H$ data are reported in the Supplemental Information as the interpretation aligns closely with the $\delta^{18}O$ data. Only $\delta^{18}O$ of WY23 precipitation ranged from -16.37 to -3.71‰ (Figure 4A). The weighted mean was -8.16‰ (SD = 2.44‰) based on the recorded precipitation amount associated with each $\delta^{18}O$ sample.

Figure 4B shows the variation of $\delta^{18}O$ values in the arroyos over the sampling period. Time period 1 included samples from winter and spring, before imported water from the SBA is released in the summer. Combined, the arroyo mean $\delta^{18}O$ values for time period 1 was -8.38‰ (SD = 0.89‰, n = 9), similar to the weighted mean of $\delta^{18}O$ value of precipitation (Table 1). Arroyo data are discussed further in the Supplemental Information. In time period 2, the summer release of imported water resulted in lower values of $\delta^{18}O$ (Table 1). Combined, the arroyo mean $\delta^{18}O$ for time period 2 was -10.87‰ (SD = 1.05‰, n = 17). Combined, the arroyo mean for time period 3 was -8.89‰ (SD = 1.26‰, n = 8), generally trending towards higher values over time (Table 1).

Three groundwater samples have $\delta^{18}O$ signatures of -2.81 to -1.29‰, which we attribute to evaporative fractionation, supported by D-excess values discussed in the Supplemental Information. The remaining 31 groundwater $\delta^{18}O$ samples ranged from -10.98‰ to -6.48 ‰ (Figure 4C). Two of these wells had $\delta^{18}O$ values less than -10‰, close to the signature of imported water. The other 29 samples from 21 wells had $\delta^{18}O$ values with a mean of -7.61‰ ($SD_{gw\text{-}local}$ = 0.62‰). These signatures are similar to the local precipitation $\delta^{18}O$ values as well as surface water $\delta^{18}O$ values from time period 1. One well, 33C1, had a $\delta^{18}O$ value of -10.2‰ during time period 2, near the range of imported water and a $\delta^{18}O$ value of -7.2‰ in time period 3, within the expected range of local precipitation when it was resampled.

3.3 ^{35}S in Source Waters and Groundwater

Precipitation and surface water samples were analyzed for ^{35}S to identify same-year recharge (WY23) in groundwater wells. We summarize these results below and show the measured activities in Figure 5.

The three precipitation samples collected in February and March of 2023 had ^{35}S activities of 2.99 ± 0.22, 3.13 ± 0.23, and 4.69 ± 0.27 mBq/L, representing 20, 5, and 33 mm of precipitation respectively. This accounts for less than 10% of the annual precipitation, a limitation discussed further in Section 4.4. Decay-corrected to July 1, the concentration of ^{35}S in precipitation ranged from 1.09 to 1.72 (± 0.1) mBq/L. Decay-corrected to October 1, ^{35}S concentrations in precipitation would have decreased to an upper value of 0.83 ± 0.05 and a lower value of 0.52 ± 0.04 mBq/L, which is near the average MDA of 0.31 mBq/L (Table 1). Groundwater samples entirely recharged by new precipitation would therefore have a detectable ^{35}S concentration, whereas we would interpret groundwater with no ^{35}S to (qualitatively) have no same-year recharge.

^{35}S was detected in 12 of 23 surface waters samples. The surface water ^{35}S activities at the time of measurement ranged from 1.0 ± 0.33 mBq/L to non-detectable values. The mean of detectable activities for all three time periods was 0.56 mBq/L (SD = 0.25 mBq/L). The detectable activities of time periods 1 and 2 were decay-corrected to July 1 and range from 0.28 ± 0.15 to 0.85 ± 0.30 mBq/L (mean = 0.54, SD = 0.22, n = 10). All detectable surface water concentrations from time period 3 were decay-corrected to October 1 and ranged from 0.9±0.32 and 0.28 ± 0.26 mBq/L (mean = 0.56, SD = 0.25, n = 12) (Table 1).

^{35}S was detected in nine out of 23 groundwater samples collected from 16 wells. The groundwater ^{35}S activities ranged from non-detectable to 1.53 mBq/L. Well 22B1 was resampled three times: ^{35}S was detected in two summer samples (0.35 ± 0.28 mBq/L and 0.56 ± 0.32 mBq/L) but not in the sample collected in the fall. Three wells (16P5, 29F4, and 33C1) were sampled twice. ^{35}S was detected in all three summer samples (1.53 ± 0.37, 1.20 ± 0.35, and 0.42 ± 0.32 mBq/L, respectively) but none had detectable ^{35}S in fall. Well 18E1 was also sampled twice, with non-detectable ^{35}S activity both times (Table 2).

3.4 ^{3}H in Source Waters and Groundwater

A total of 37 ^{3}H samples were analyzed to understand groundwater transit times, the results of which are summarized below.

Potential sources of recharge (precipitation and surface waters) had indistinguishable ^{3}H activities. Tritium in precipitation ranged from 5.34 ± 0.30 to 12.56 ± 0.60 pCi/L (mean = 9.0, SD = 2.2 pCi/L, n = 5). The lowest concentration (5.34 pCi/L) was measured in a sample representing a large single-day precipitation event on January 1, 2023. The precipitation weighted mean concentration was 8.2 pCi/L (Table 1). Tritium in arroyo waters varied from 7.59±0.57 to 10.32 ± 0.45 pCi/L (mean = 8.44, SD = 0.78 pCi/L, n = 11) in winter and spring (Time period 1), and 10.47 ± 0.56 pCi/L (n = 1) in summer (Time period 2). One additional sample representing the natural arroyo stream signatures (collected upstream of the imported water input) had a lower ^{3}H activity of 5.93 ± 0.55 pCi/L. Two samples from Time period 3 had ^{3}H activities of 8.10 ± 0.63 and 8.63 ± 0.63 pCi/L (Table 1).

Out of 5 groundwater samples, two (16P5, 9.37 ± 0.55 pCi/L; 33C1, 7.51 ± 1.30 pCi/L) were within measurement error of all three sources (Table 2). One groundwater sample (26J2, 6.83 ± 0.75 pCi/L) represents either a mixture of new recharge and older water, or water that entirely recharged before 2023. One well sample (29F4) had a low tritium concentration (1.52 ± 0.65 pCi/L), which, assuming an initial ^{3}H tritium concentration of 8.2 pCi/L (from the measured local precipitation), indicates a travel time of 24-43 years. One well sample (18E1) did not contain tritium above the detection limit (1 pCi/L) which indicates it recharged entirely before the 1950s.

4. DISCUSSION

The discussion section is organized around three objectives: (1) characterize the combined isotopic signature of potential recharge sources, (2) identify the source of recharge to groundwater in the Livermore basin, particularly new recharge, and (3) analyze the land use surrounding wells that receive new recharge.

4.1 Characterizing the Isotopic Signatures of Potential Recharge Waters

First, $\delta^{18}O$ monitoring enabled us to distinguish local versus imported water as potential sources of recharge. Using the precipitation $\delta^{18}O$ and the temporal variation of $\delta^{18}O$ in surface waters, we describe two primary sources of water. Local precipitation, including natural flow arroyo waters, is characterized by the $\delta^{18}O$ values ranging from -10‰ to -5‰, based on the precipitation weighted mean and mean values of the arroyos in time period 1. Imported arroyo waters are characterized by $\delta^{18}O$ values below -10‰, based on surface water $\delta^{18}O$ values in time period 2.

In September and October (during time period 3), $\delta^{18}O$ values in AM and AV waters increase, which may indicate mixing of imported and local precipitation due to a larger component of locally recharged groundwater discharge, or evaporation of surface waters (thereby increasing $\delta^{18}O$ values) through the dry season. Electrical conductivity values of these waters also trend slightly higher during this time, which supports the interpretation of increasing evaporation during these months and the potential for local groundwater discharge (see Supplementary Information for more details).

Because the $\delta^{18}O$ signatures of wintertime arroyo waters and local precipitation from WY23 are identical, $\delta^{18}O$ values cannot distinguish between these two sources. In contrast, the difference in $\delta^{18}O$ values between arroyo water during time period 1 (winter and spring, runoff from the local watershed) and arroyo water during time period 2, (representing the influx of water imports to the arroyos) is 2.5‰. This difference is larger than the combined $\delta^{18}O$ uncertainty of the two recharge source types (local versus imported) (1.94‰) which enables a clear distinction of the source of recharge to nearby wells.

While the source of arroyo waters in time period 1 (January-June 2023) is aligned with a local precipitation source according to the $\delta^{18}O$ signature, the low ^{35}S activity in the arroyos suggests that arroyo samples in time period 1 contain a large proportion of "older" water (in the qualitative context of ^{35}S, this is limited to mean water which fell as precipitation some time prior to WY23). This is consistent with the low ^{3}H concentration (5.93 ± 0.55 pCi/L) in the sample collected in July 2023 from higher up in the watershed of AM (upstream of the imported water input) in which ^{35}S was not detected.

In time period 2 and 3, July through October 2023, more frequent detections of ^{35}S activity in arroyo surface water indicate, qualitatively, some detectable proportion of WY23 precipitation in the streams, more frequently than in time period 1. In the same period $\delta^{18}O$ values were also gradually increasing towards local precipitation values.

We summarize the combined isotopic signatures in Table 1 to describe the potential recharge inputs to the Zone 7 Groundwater Basin. The higher precipitation ^{35}S activities enable distinction between direct precipitation recharge and surface water recharge in time period 1 (winter and spring) when both sources have high $\delta^{18}O$ values. In time period 2, the low $\delta^{18}O$ signature of imported water enables the distinction from local recharge. In time period 3 (after Oct 1^{st}), decay of ^{35}S resulted in low concentrations in direct recharge of local precipitation, which are now similar to arroyo waters in this period. In this time period 3, winter arroyo recharge and prior year recharge will both have non-detectable ^{35}S activities.

We decay-corrected ^{35}S data from precipitation and surface waters to enable direct comparisons with groundwaters. Groundwater samples collected in time period 2 are compared to precipitation and surface waters from time periods 1 and 2. For this comparison, the lowest concentration of ^{35}S in precipitation, decay-corrected to 1 July 2023, is 1.09 ± 0.09 mBq/L whereas the highest concentration of ^{35}S in local arroyo waters, decay-corrected to 1 July 2023, is 0.55 ± 0.22 mBq/L. This difference of 0.23 to 0.41 mBq/L (accounting for measurement errors) enables the distinction between these two sources, which are similar in $\delta^{18}O$ and ^{3}H values. Imported arroyo waters in time period 2 have distinctly lower $\delta^{18}O$ signatures.

Groundwaters collected during time period 3 are compared to precipitation and surface water signatures from all time periods. The lowest concentration of ^{35}S in precipitation, decay-corrected to 1 October 2023, is 0.52 mBq/L whereas the highest concentration of ^{35}S in arroyo waters, decay-corrected to 1 October 2023, is below the typical detection limit (0.26 mBq/L). This difference enables the distinction between these two sources, which are similar in $\delta^{18}O$ and ^{3}H. Imported arroyo waters still have distinctly lower $\delta^{18}O$ signatures. However, arroyo waters in this time period have ^{35}S concentrations up to 0.9 mBq/L. That makes it impossible to distinguish arroyo recharge in this period from direct precipitation recharge in winter.

4.2 Detecting Flood-MAR in the Livermore Valley Groundwater Basin

We combined $\delta^{18}O$, ^{3}H, and ^{35}S analyses from 16 wells in Figure 6 to identify the likely source water of each groundwater sample (Table 2).

Infiltration of WY23 precipitation (n=3): Of the 9 wells sampled during July 2023, three wells (26J2, 16P5, and 33C1) yielded ^{35}S activities above 0.99 ± 0.35 mBq/L. These ^{35}S activities are higher than the highest ^{35}S activities found in arroyo waters, making it unlikely that the arroyos are the sole source of recharge. The similarity with precipitation concentrations suggests that these samples have a large proportion of WY23 precipitation recharge.

The source of water in two of the three wells, 26J2 ($\delta^{18}O$ = -7.18‰ in July) and16P5 ($\delta^{18}O$ =-7.55‰ in June, -8.24‰ in October) is local precipitation (Table 2). These two wells were categorized with mixed and modern ^{3}H-interpreted age categories, respectively, further supporting the interpretation that they receive a portion of rapid recharge. This combination of signatures indicates that direct infiltrations of new WY23 precipitation is the source of recharge to these wells.

In contrast, the $\delta^{18}O$ value of 33C1, which has a screened interval depth from 1.5 to 6 m, varied from -10.18‰ in July (when ^{35}S was detectable) to -7.22‰ in November (when ^{35}S was not detected). We attribute the variation in $\delta^{18}O$ values to very rapid recharge of precipitation with insufficient time for dispersion and mixing to smooth the variability of $\delta^{18}O$ in precipitation or to a change in recharge source from imported waters to locally sourced natural flow. This is supported by the modern ^{3}H signature.

Infiltration of WY23 precipitation mixed with ambient groundwater (n=3): Three wells (20C8, 22B1, 29F4) yielded detectable, but lower ^{35}S activities, not necessarily overlapping with the expected ^{35}S activity of precipitation. Given the non-detectable decay-corrected ^{35}S activities for natural arroyo waters, we interpret these samples to have a component of direct infiltration of local precipitation. 22B1 was sampled three times, with detectable ^{35}S activities in June and July, and no detectable ^{35}S activity in fall. We interpret this result as young water mixing with pre-WY23 (low ^{35}S activity) waters. Alternatively, the decrease in ^{35}S activity is due to ^{35}S decay over approximately one half-life between samples. Combining this interpretation with the $\delta^{18}O$ value of local precipitation source signals ($\delta^{18}O$ > -8‰), these wells likely represent a mixture of young and old local water due to dispersion within the groundwater flow paths. Well 29F4 had a ^{3}H-interpreted age category of mixed ages.

The detection of ^{35}S (0.73 ± 0.30 mBq/L) in well 20C8 is notable because ^{35}S was not detected in well 20C7, a well from the same location with a shallower screened interval (20-44 m depth), where 20C8 has a screened interval from 90 to 96 m depth. Both wells were sampled in July. The 20C8 sample is from the Lower Aquifer, the Upper Livermore Formation, and there is thought to be an aquitard separating it from Upper (alluvial) Aquifer from which the 20C7 samples was taken. There may be channels of gravel between the two screened sections, however the well log lithological description does record clay in between these screened intervals.

Pond recharge with evaporated $\delta^{18}O$ (n = 2): The two wells (10N2 and 10N3) with high $\delta^{18}O$ values ($\delta^{18}O$>-3‰), indicative of evaporated water, are likely sourced from water infiltrating from nearby gravel quarry ponds (Figure 1A). Low but detectable ^{35}S activities in these wells indicate that WY23 precipitation mixed in the settling ponds and then infiltrated the local aquifer.

Local pre-WY23 recharge (n=7): We characterize seven wells (18E2, 19N3, 19N4, 20C7, 22D2, 23E2, and 6E4) as local, pre-WY23 recharge based on $\delta^{18}O$ signatures within the range of local precipitation (-6.5 to -8.7 ‰) and non-detectable ^{35}S activities. Non-detectable tritium in well 18E2 indicates pre-modern recharge, eliminating recharge from arroyos in time period 1 as a possibility.

Imported arroyo water recharge (n=1): Well 33G1 had a $\delta^{18}O$ value ($\delta^{18}O$ = -11‰) similar to imported arroyo waters recharged primarily from summer SBA releases in time period 2. The non-detectable ^{35}S activity is consistent with non-detectable results in the arroyos in this period.

4.3 Spatial Variation of Recharge Along the Arroyo

Wells in the upper sections of the arroyo, especially above the SBA input, are surrounded by open space that includes natural reserves and agriculture. While we expected younger water (faster recharge) to be found in these upstream regions where the alluvial aquifer is thin and the wells are shallow, we did not find evidence in the collected isotopic data. Instead, the distribution of water sources and isotope-derived ages varies across the study area (Figure 7). Lateral distance and well depth did not correlate with water source or isotopic age (more detail in the

Supplemental Information). It is possible that sediment channels of coarse grained materials may provide "fast paths" between surface waters and sampled wells, but this was not able to be determined with lithologies in well construction records, discussed further in the Supplemental Information. Overall, our results suggest that recharge along the arroyo is more heterogeneous than indicated by current modelling.

Wells with recent recharge (16P5, 26J2) are in agricultural land and an urban park, whereas the wells with non-detectable ^{35}S are found in more highly paved areas. We conclude the surrounding open space enabled fast infiltration of local precipitation.

In contrast, well 33C1 was interesting because of its young recharge (high ^{35}S and ^{3}H activities), as well as a variable water source. This well is close to the diversion point for SBA imported water, which may contribute to the rapid change in water source, suggesting that the arroyo channel is responsible as a mechanism of recharge in this location. The other well close to the SBA input in AM (26J2) had young water but did not show a change in source during the study period.

The location of these three young wells is notable because they are in unpaved, open spaces even within an urban area. These might be important recharge sites as well as providing urban green spaces, which are also associated with social co-benefits (Barron et al., 2019; Chen et al., 2019; Kingsley & EcoHealth, 2019).

Inactive gravel mine ponds are sources of groundwater recharge, containing a mix of diverted water, local precipitation, and flood waters. Two wells that are close to these mine ponds (and more than 1 km away from the arroyo) show evidence of new recharge and of evaporative fractionation. This combination suggests that the mine settling ponds are the source of water for these wells.

Seven wells have no evidence of recent recharge. They are all within 170 m of the arroyos, some as close as 50 m, and within 65 m below ground surface, some as shallow as 20 m, both along the upper reaches of the arroyos and in the lower basin. These data points suggest that arroyo recharge is localized and help refine our understanding of groundwater recharge in the basin.

4.4 Limitations and Transferability

This study provides promising applications for combined isotopic analysis in highly managed aquifers. We found that ^{35}S can distinguish precipitation from surface waters recharged in the winter and spring seasons. Consequently, the connections to groundwater recharge may be better identified with early-season (winter and spring) groundwater sampling, if very rapid recharge is occurring.

The combined analyses of $\delta^{18}O$, ^{35}S, and ^{3}H signatures supported our understanding of the timing of recharge from local water via flood-MAR. ^{35}S may be less applicable at MAR facilities supplied by imported waters that contain a larger proportion of water from prior water years, because initial concentrations are too low to distinguish sources or calculate ages, also noted in previous urban MAR studies (Clark et al., 2016).

The methods developed here provide the basis for further investigation of the mechanisms or sites for urban groundwater recharge (ponds, arroyo floodplains, and dispersed recharge in open spaces). The relationship between open, unpaved spaces and groundwater recharge in both agricultural and urban environments can also be better constrained with additional sampling in paved and relatively more permeable land surface areas. These techniques, carefully applied, can identify regions with high potential for groundwater recharge, highlighting the importance for land-use decision-making for sustainable water management and compliance with legislation such as SGMA.

If a single recharge source and ^{35}S activity from the MAR basin infiltration can be assumed, transit times between the recharge source and sample collection point can be calculated (Clark et al., 2016; Schubert et al., 2020; Urióstegui et al., 2017; Yoon et al., 2023). Due to the potential for multiple source waters and mixing, precise transit time calculations are not feasible in this setting.

Three precipitation samples from WY23 are not enough to capture the uncertainty in the potential precipitation inputs to the surface and groundwater systems. High precipitation rates in WY23 (600 mm, 170% of the average annual precipitation) likely resulted in lower ^{35}S activity in precipitation due to dilution, limiting the applicability of ^{35}S as a tracer (Schubert et al., 2020; Schubert et al., 2021). A prior reconstruction of ^{35}S in precipitation calculated a precipitation-weighted mean value of 24.2 mBq/L for a research site in the Sierra Nevada, 300 km southeast of Livermore at an elevation of 2 km, with sample concentrations ranging from 3 to 103 mBq/L (Visser et al., 2019). The high elevation and greater distance to the Pacific Ocean are likely causes for higher ^{35}S activities at that location. Subsequent measurements of local Livermore precipitation in WY24 also indicate higher ^{35}S activities in precipitation, with a precipitation-weighted mean of 9.2 mBq/L (discussed further in the Supplemental Information). Higher input (precipitation) concentrations may have resulted in more detections in groundwater and lower relative uncertainties around measured concentrations. They would furthermore enable quantifying mixing ratios with associated uncertainties. However, the drivers of the ^{35}S production and deposition are insufficiently known to accurately reconstruct WY23 precipitation activities.

^{35}S concentrations in the arroyo samples were lower than expected, despite the high flow rates in response to precipitation events. Despite the drought years preceding WY23, it appears arroyo waters contained a large proportion of water that fell as precipitation in prior water years. Low proportions of new water (30% on average) were also found in a steep research catchment in the Sierra Nevada (Visser et al., 2019). Average ^{35}S activities in that watershed ranged from 6% to 28% of the ^{35}S activity measured in precipitation. ^{35}S as a tracer of MAR water appears to be limited to situations with relatively high inputs and limited contributions of local precipitation recharge, such as the MAR facilities in the Los Angeles basin (Clark et al., 2016; Urióstegui et al., 2017); however, it can be a sensitive tracer to identify local precipitation recharge, illustrating how land use enables infiltration of extreme precipitation events.

5. CONCLUSION

A combination of natural isotopic tracers allows for a reconstruction of recharge mechanisms. Direct infiltration of precipitation can be detected in groundwater thanks to high ^{35}S concentrations in precipitation. However, low ^{35}S activities in arroyo waters complicate the distinction between stream infiltration and ambient (pre-WY23) groundwater. Differences in $\delta^{18}O$ between imported and local water allow for reliable source identification. Additional age tracer data (e.g. ^{3}H) helps confirm the presence or absence of new infiltration. It should be noted that monitoring the signatures in all possible recharge sources (e.g. surface waters and precipitation) is necessary when source signatures are variable, either naturally or due to management actions.

Recharge is heterogeneous. Isotopic contrasts at short distances and a lack of consistent patterns with depth or distance to arroyos illustrate the complexity of recharge. This complexity needs to be incorporated in scientific and operational models of groundwater recharge to make reliable predictions of how groundwater basins will respond to climate impacts on precipitation and flooding.

In conclusion, ^{35}S is a promising isotope system for identifying infiltration of local precipitation, particularly in situations where permeable surfaces are installed as MAR mechanisms. The short half-life of ^{35}S allows for the identification and quantification of new recharge in complex settings, where seasonal variation in $\delta^{18}O$ is unpredictable and residence times are too short for ^{3}H age determination. Water managers can implement these tools on a broad scale to better understand the interaction between groundwater and surface water, optimize infiltration, and protect groundwater dependent ecosystems. Water managers and researchers alike can benefit from ^{35}S analyses in settings with water augmentation to understand fast recharge pathways.

6. ACKNOWLEDGMENTS

Part of this work was performed under the auspices of the U.S. Department of Energy by Lawrence Livermore National Laboratory under Contract DE-AC52-07NA27344, with funding from the Laboratory Directed Research and Development (LDRD) program (23-ERD-039).

LLNL-JRNL-865947. We thank Dr. M. Smith for collecting precipitation samples in Livermore for water stable isotope analysis.

DATA AVAILABILITY

Research Data associated with this article are included in Supplementary Information Tables S1-S8.

REFERENCES

Águila, J. F., Samper, J., & Pisani, B. (2019). Parametric and numerical analysis of the estimation of groundwater recharge from water-table fluctuations in heterogeneous unconfined aquifers. *Hydrogeology Journal*, *27*(4), 1309-1328. https://doi.org/10.1007/s10040-018-1908-x

Akyuz, F. A. (2017). *Drought Severity and Coverage Index. United States Drought Monitor.* https://droughtmonitor.unl.edu/About/AbouttheData/DSCI.aspx

Barron, S., Nitoslawski, S., Wolf, K. L., Woo, A., Desautels, E., & Sheppard, S. R. J. (2019). Greening Blocks: A Conceptual Typology of Practical Design Interventions to Integrate Health and Climate Resilience Co-Benefits. *Int J Environ Res Public Health*, *16*(21). https://doi.org/10.3390/ijerph16214241

Brothers, L. A., Dominguez, G., Abramian, A., Corbin, A., Bluen, B., & Thiemens, M. H. (2010). Optimized low-level liquid scintillation spectroscopy of 35S for atmospheric and biogeochemical chemistry applications. *Proc Natl Acad Sci U S A*, *107*(12), 5311-5316. https://doi.org/10.1073/pnas.0901168107

Carlson, M. A., Lohse, K. A., McIntosh, J. C., & McLain, J. E. T. (2011). Impacts of urbanization on groundwater quality and recharge in a semi-arid alluvial basin. *Journal of Hydrology*, *409*(1-2), 196-211. https://doi.org/10.1016/j.jhydrol.2011.08.020

Carpenter, D. W., Sweeney, J. J., Kasameyer, P. W., Burkhard, N. R., Knauss, K. G., & Shlemon, R. J. (1984). *Geology of the Lawrence Livermore National Laboratory site and adjacent areas* (UCRL-53316).

Chen, L.-M., Chen, J.-W., Chen, T.-H., Lecher, T., & Davidson, P. (2019). Measurement of Permeability and Comparison of Pavements. *Water*, *11*(3). https://doi.org/10.3390/w11030444

CIMIS. (2024). *California Irrigation Management Information System. CIMIS Monthly Average ETo Report: Pleasanton* https://cimis.water.ca.gov/UserControls/Reports/MonthlyEtoReportViewer.aspx

Clark, I. D., & Fritz, P. (1997). *Environmental Isotopes in Hydrogeology Environmental Isotopes in Hydrogeology* CRC press.

Clark, J., Urióstegui, S., Bibby, R., Esser, B., & Tredoux, G. (2016). Quantifying Apparent Groundwater Ages near Managed Aquifer Recharge Operations Using Radio-Sulfur (35S) as an Intrinsic Tracer. *Water*, *8*(11). https://doi.org/10.3390/w8110474

Clarke, W. B., Jenkins, W. J., & Top, Z. (1976). Determination of tritium by mass spectrometric measurement of 3He. *The international journal of applied radiation and isotopes*, *27*(9), 515-522.

Coplen, T. B. (1995). Reporting of stable hydrogen, carbon, and oxygen isotopic abundances. *Geothermics*, *5*(24), 707-712.

Council, N. R. M. M. (2009). *Australian guidelines for water recycling: Managing health and environmental risks (phase 2), managed aquifer recharge.* (National Water Quality Management Strategy Document no 24., Issue.

Currie, L. A. (1968). Limits for qualitative detection and quantitative determination. Application to radiochemistry. *Analytical chemistry*, *40*(3), 586-593.

Deinhart, A. L., Bibby, R. K., Visser, A., Thaw, M., & Thomas, K. (2021). Simplified Method for the In Situ Collection and Laboratory Analysis of Cosmogenic Tracers (Sulfur-35 and Sodium-22) to Determine Residence Time Distributions and Water Ages. *Anal Chem*, *93*(10), 4472-4478. https://doi.org/10.1021/acs.analchem.0c04490

Di Renzo, D., Rizzo, A., Telloli, C., Salvi, S., Marrocchino, E., Nieto Yabar, D., & Vaccaro, C. (2023). Geochemical and isotopic tracers to define the aquifer's vulnerability: the case study of the alluvial multi-aquifer system of the Friulian plain. *Environ Monit Assess*, *195*(6), 781. https://doi.org/10.1007/s10661-023-11359-7

Dillon, P. (2005). Future management of aquifer recharge. *Hydrogeology Journal*, *13*(1), 313-316. https://doi.org/10.1007/s10040-004-0413-6

Dillon, P., Stuyfzand, P., Grischek, T., Lluria, M., Pyne, R. D. G., Jain, R. C., Bear, J., Schwarz, J., Wang, W., Fernandez, E., Stefan, C., Pettenati, M., van der Gun, J., Sprenger, C., Massmann, G., Scanlon, B. R., Xanke, J., Jokela, P., Zheng, Y., . . . Sapiano, M. (2018). Sixty years of global progress in managed aquifer recharge. *Hydrogeology Journal*, *27*(1), 1-30. https://doi.org/10.1007/s10040-018-1841-z

Hartzell, S., Leeds, A. L., Ramirez-Guzman, L., Allen, J. P., & Schmitt, R. G. (2016). Seismic Site Characterization of an Urban Sedimentary Basin, Livermore Valley, California: Site Response, Basin-Edge-Induced Surface Waves, and 3D Simulations. *Bulletin of the Seismological Society of America*, *106*(2), 609-631. https://doi.org/10.1785/0120150289

IGRAC. (2016). *International Groundwater Resources Assessment Centre, Global MAR inventory*. Retrieved Feb 24 from https://ggis.un-igrac.org/view/marportal/

Jameel, Y., Brewer, S., Fiorella, R. P., Tipple, B. J., Terry, S., & Bowen, G. J. (2018). Isotopic reconnaissance of urban water supply system dynamics. *Hydrology and Earth System Sciences*, *22*(11), 6109-6125. https://doi.org/10.5194/hess-22-6109-2018

Joël Casanova, N. D., and Marie Pettenati. Managed Aquifer Recharge: An Overview of Issues and Options. In O. B. Anthony J. Jakeman, Randall J. Hunt, Jean-Daniel Rinaudo, Andrew Ross (Ed.), *Integrated Groundwater Management* (pp. 413-434). Springer International Publishing https://doi.org/10.1007/978-3-319-23576-9_16

Kingsley, M., & EcoHealth, O. (2019). Commentary - Climate change, health and green space co-benefits. *Health Promot Chronic Dis Prev Can*, *39*(4), 131-135. https://doi.org/10.24095/hpcdp.39.4.04 (Commentaire - Changements climatiques, sante et avantages connexes des espaces verts.)

Kirchner, J. W. (2019). Quantifying new water fractions and transit time distributions using ensemble hydrograph separation: theory and benchmark tests. *Hydrology and Earth System Sciences*, *23*(1), 303-349. https://doi.org/10.5194/hess-23-303-2019

Klaus, J., & McDonnell, J. J. (2013). Hydrograph separation using stable isotopes: Review and evaluation. *Journal of Hydrology*, *505*, 47-64. https://doi.org/10.1016/j.jhydrol.2013.09.006

Kuang, X., Liu, J., Scanlon, B. R., Jiao, J. J., Jasechko, S., Lancia, M., Biskaborn, B. K., Wada, Y., Li, H., Zeng, Z., Guo, Z., Yao, Y., Gleeson, T., Nicot, J. P., Luo, X., Zou, Y., & Zheng, C. (2024). The changing nature of groundwater in the global water cycle. *Science*, *383*(6686), eadf0630. https://doi.org/10.1126/science.adf0630

Kundzewicz, Z. W., & Döll, P. (2009). Will groundwater ease freshwater stress under climate change? *Hydrological Sciences Journal*, *54*(4), 665-675. https://doi.org/10.1623/hysj.54.4.665

Lindsey, B. D., Jurgens, B. C., & Belitz, K. *Tritium as an Indicator of Modern, Mixed, and Premodern Groundwater Age*.
Mamand, B. S., & Mawlood, D. K. (2023). Estimating Mean Residence Time of Groundwater in Central Basin/Erbil using Environmental Isotopes. *Zanco Journal of Pure and Applied Sciences*, *35*(3), 39-46. https://doi.org/10.21271/zjpas
Marr, J., Dhillon, D., Arrate, D., Stygar, S., & Maendly, R. (2018). *FLOOD-MAR: Using Flood Water for Managed Aquifer Recharge to Support Sustainable Water Resources*.
Marx, C., Tetzlaff, D., Hinkelmann, R., & Soulsby, C. (2021). Isotope hydrology and water sources in a heavily urbanized stream. *Hydrological Processes*, *35*(10). https://doi.org/10.1002/hyp.14377
Michel, & Natfz. (1995). Use of sulfur-35 and tritium to study runoff from an alpine glacier, Wind River Range, Wyoming.
Moore, K. B., Ekwurzel, B., Esser, B. K., Hudson, G. B., & Moran, J. E. (2006). Sources of groundwater nitrate revealed using residence time and isotope methods. *Applied Geochemistry*, *21*(6), 1016-1029. https://doi.org/10.1016/j.apgeochem.2006.03.008
Moran, J. E., Hudson, G. B., Eaton, G. F., & Leif, R. (2002). *A Contamination Vulnerability Assessment for the Livermore-Amador and Niles Cone Groundwater Basins*.
Poluianov, S. V., Kovaltsov, G. A., & Usoskin, I. G. (2020). A New Full 3-D Model of Cosmogenic Tritium 3H Production in the Atmosphere (CRAC:3H). *Journal of Geophysical Research: Atmospheres*, *125*(18). https://doi.org/10.1029/2020jd033147
PRISM, C. G. (2014). *PRISM Climate Group, PRISM Climate Data*. Oregon State University. https://prism.oregonstate.edu
Priyadarshi, A., Hill-Falkenthal, J., Thiemens, M., Zhang, Z., Lin, M., Chan, C. y., & Kang, S. (2014). Cosmogenic 35S measurements in the Tibetan Plateau to quantify glacier snowmelt. *Journal of Geophysical Research: Atmospheres*, *119*(7), 4125-4135. https://doi.org/10.1002/2013jd019801
Ringleb, J., Sallwey, J., & Stefan, C. (2016). Assessment of Managed Aquifer Recharge through Modeling—A Review. *Water*, *8*(12). https://doi.org/10.3390/w8120579
Schubert, M., Knöller, K., Tegen, I., & Terzi, L. (2020). Variability of Cosmogenic 35S in Rain—Resulting Implications for the Use of Radiosulfur as Natural Groundwater Residence Time Tracer. *Water*, *12*(10). https://doi.org/10.3390/w12102953
Schubert, M., Weise, S. M., & Knoller, K. (2021). Atmospheric washout of (35)S during single rain events - Implications for (35)S sampling schemes. *J Environ Radioact*, *237*, 106669. https://doi.org/10.1016/j.jenvrad.2021.106669
Shanley, J. B., Mayer, B., Mitchell, M. J., Michel, R. L., Bailey, S. W., & Kendall, C. (2005). Tracing Sources of Streamwater Sulfate During Snowmelt Using S and O Isotope Ratios of Sulfate and 35S Activity. *Biogeochemistry*, *76*(1), 161-185. https://doi.org/10.1007/s10533-005-2856-9
Siirila-Woodburn, E. R., Rhoades, A. M., Hatchett, B. J., Huning, L. S., Szinai, J., Tague, C., Nico, P. S., Feldman, D. R., Jones, A. D., Collins, W. D., & Kaatz, L. (2021). A low-to-no snow future and its impacts on water resources in the western United States. *Nature Reviews Earth & Environment*, *2*(11), 800-819. https://doi.org/10.1038/s43017-021-00219-y
Surano, K., Hudson, G., Failor, R., Sims, J., Holland, R., MacLean, S., & Garrison, J. (1992). Heliuim-3 mass spectrometry for low-level tritium analysis of environmental samples. *Journal of radioanalytical and nuclear chemistry*, *161*(2), 443-453.
Telloli, C., Rizzo, A., Salvi, S., Pozzobon, A., Marrocchino, E., & Vaccaro, C. (2022). Characterization of groundwater recharge through tritium measurements. *Advances in Geosciences*, *57*, 21-36. https://doi.org/10.5194/adgeo-57-21-2022

Tetzlaff, D., Buttle, J., Carey, S. K., McGuire, K., Laudon, H., & Soulsby, C. (2014). Tracer-based assessment of flow paths, storage and runoff generation in northern catchments: a review. *Hydrological Processes*, *29*(16), 3475-3490. https://doi.org/10.1002/hyp.10412

Tolstikhin, I. N., & Kamenski, I. L. (1969). Determination of groundwater age by the T-3He method. *Geochemistry International*, *6*, 810-811.

Ulibarri, N., Escobedo Garcia, N., Nelson, R. L., Cravens, A. E., & McCarty, R. J. (2021). Assessing the Feasibility of Managed Aquifer Recharge in California. *Water Resources Research*, *57*(3). https://doi.org/10.1029/2020wr029292

Uriostegui, S. H., Bibby, R. K., Esser, B. K., & Clark, J. F. (2015). Analytical Method for Measuring Cosmogenic (35)S in Natural Waters. *Anal Chem*, *87*(12), 6064-6070. https://doi.org/10.1021/acs.analchem.5b00584

Urióstegui, S. H., Bibby, R. K., Esser, B. K., & Clark, J. F. (2017). Quantifying annual groundwater recharge and storage in the central Sierra Nevada using naturally occurring35S. *Hydrological Processes*, *31*(6), 1382-1397. https://doi.org/10.1002/hyp.11112

Visser, A., Moran, J. E., Hillegonds, D., Singleton, M. J., Kulongoski, J. T., Belitz, K., & Esser, B. K. (2016). Geostatistical analysis of tritium, groundwater age and other noble gas derived parameters in California. *Water Res*, *91*, 314-330. https://doi.org/10.1016/j.watres.2016.01.004

Visser, A., Moran, J. E., Singleton, M. J., & Esser, B. K. (2018). Importance of river water recharge to the San Joaquin Valley groundwater system. *Hydrological Processes*, *32*(9), 1202-1213. https://doi.org/10.1002/hyp.11468

Visser, A., Thaw, M., Deinhart, A., Bibby, R., Safeeq, M., Conklin, M., Esser, B., & Van der Velde, Y. (2019). Cosmogenic Isotopes Unravel the Hydrochronology and Water Storage Dynamics of the Southern Sierra Critical Zone. *Water Resources Research*, *55*(2), 1429-1450. https://doi.org/10.1029/2018wr023665

Xia, C., Liu, Y., Meng, Y., Liu, G., Huang, X., Chen, Y., & Chen, K. (2023). Stable isotopes reveal the surface water-groundwater interaction and variation in young water fraction in an urbanized river zone. *Urban Climate*, *51*. https://doi.org/10.1016/j.uclim.2023.101641

Ye, S., Liu, L., Chen, X., Li, P., Xu, G., & Ran, Q. (2022). The Variability of Stable Water Isotopes and the Young Water Fraction in a Mountainous Catchment. *CLEAN – Soil, Air, Water*, *50*(7). https://doi.org/10.1002/clen.202100337

Yoon, Y. Y., Ko, K. S., & Lee, J. M. (2023). Tritium and 35S activity variation in precipitation in Korea and its application to groundwater age determination. *Journal of radioanalytical and nuclear chemistry*, *332*(6), 1917-1921. https://doi.org/10.1007/s10967-023-08888-3

Zhang, H., Xu, Y., & Kanyerere, T. (2020). A review of the managed aquifer recharge: Historical development, current situation and perspectives. *Physics and Chemistry of the Earth, Parts A/B/C*, *118-119*. https://doi.org/10.1016/j.pce.2020.102887

Zone 7. (2023). *Zone 7 Water Agency. Livermore Valley Groundwater Basin Sustainable Groundwater Management Annual Report 2022 Water Year (October 2021 – September 2022)*.

FIGURES

Figure 1. A) Map of Livermore Amador Valley showing the two arroyos (Arroyo Mocho and Arroyo Valle) flowing from the southeast to the west. B) Map of sample locations, with relevant hydrologic features marked such as the South Bay Aqueduct (SBA) and Reservoir Del Valle, as well as generalized rock types of the Livermore Groundwater Basin. Groundwater well names are labelled.

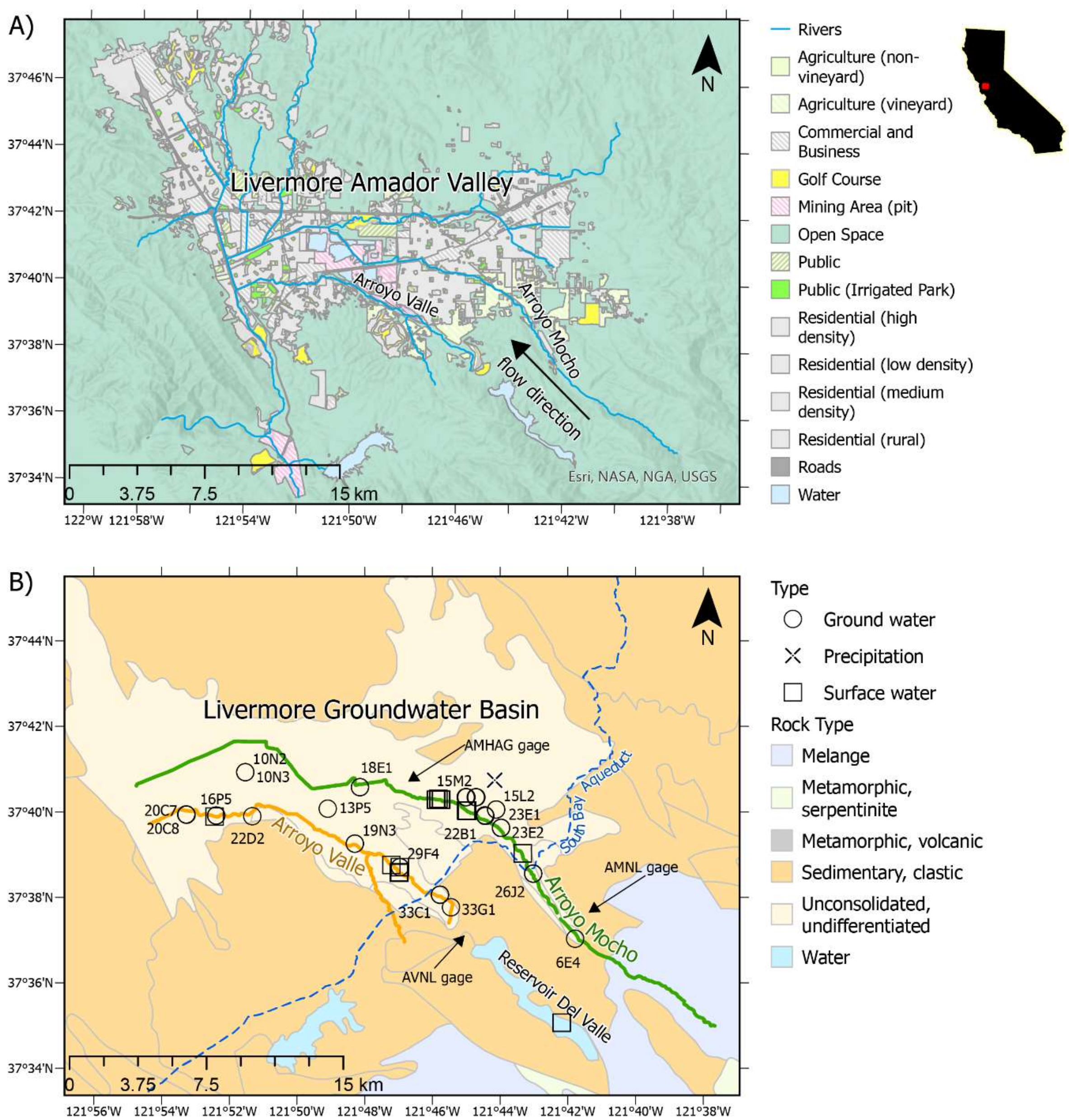

Figure 2. Hydrologic information including A) rainfall, and B) modelled groundwater recharge for the Livermore Groundwater Basin from Water Year 1974-2023 (Zone 7, 2023).

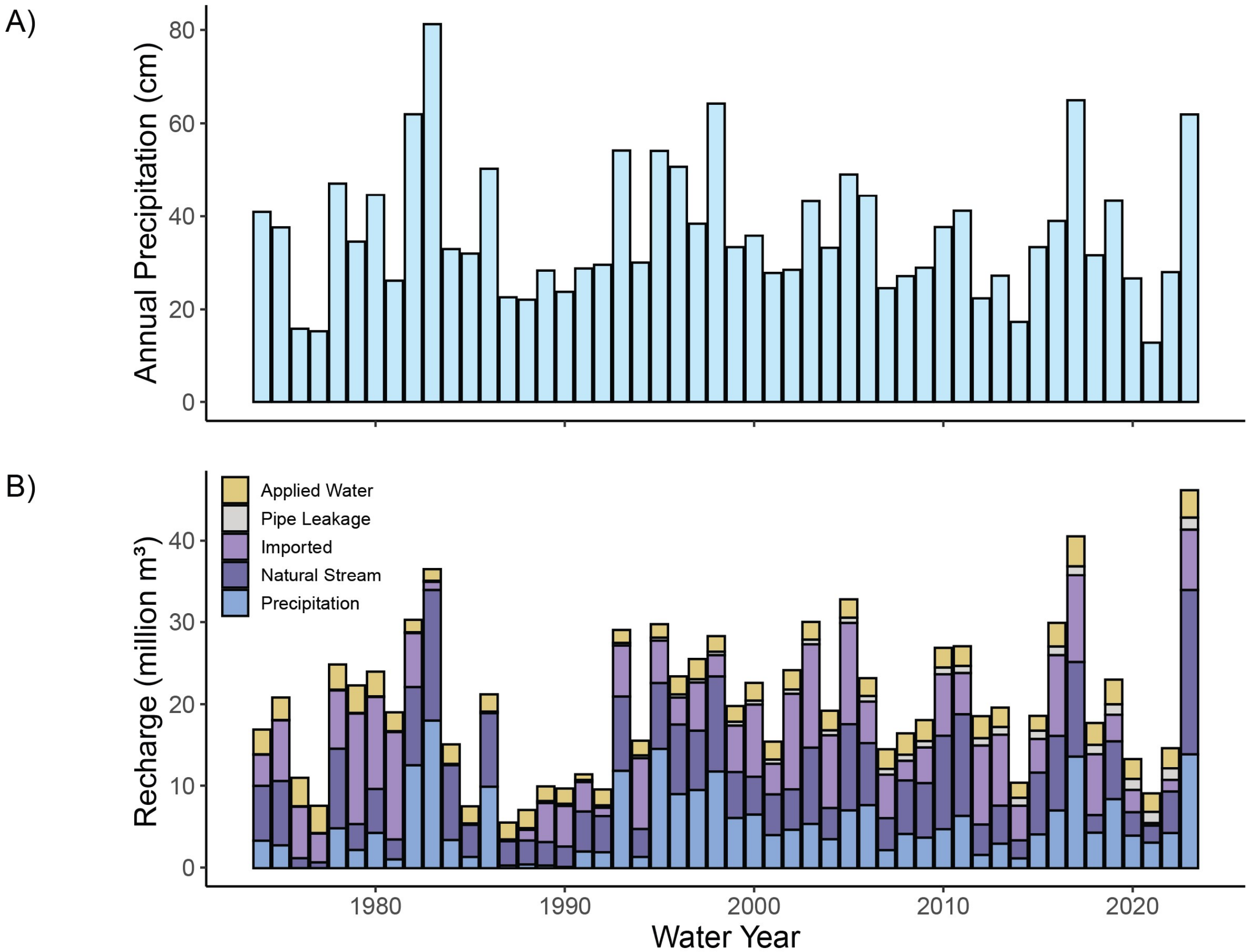

Figure 3. Stream water information in WY23. A) Daily discharge measurements at arroyos B) AM water source distribution by day, where white areas indicate no flow. C) AV water source distribution by day.

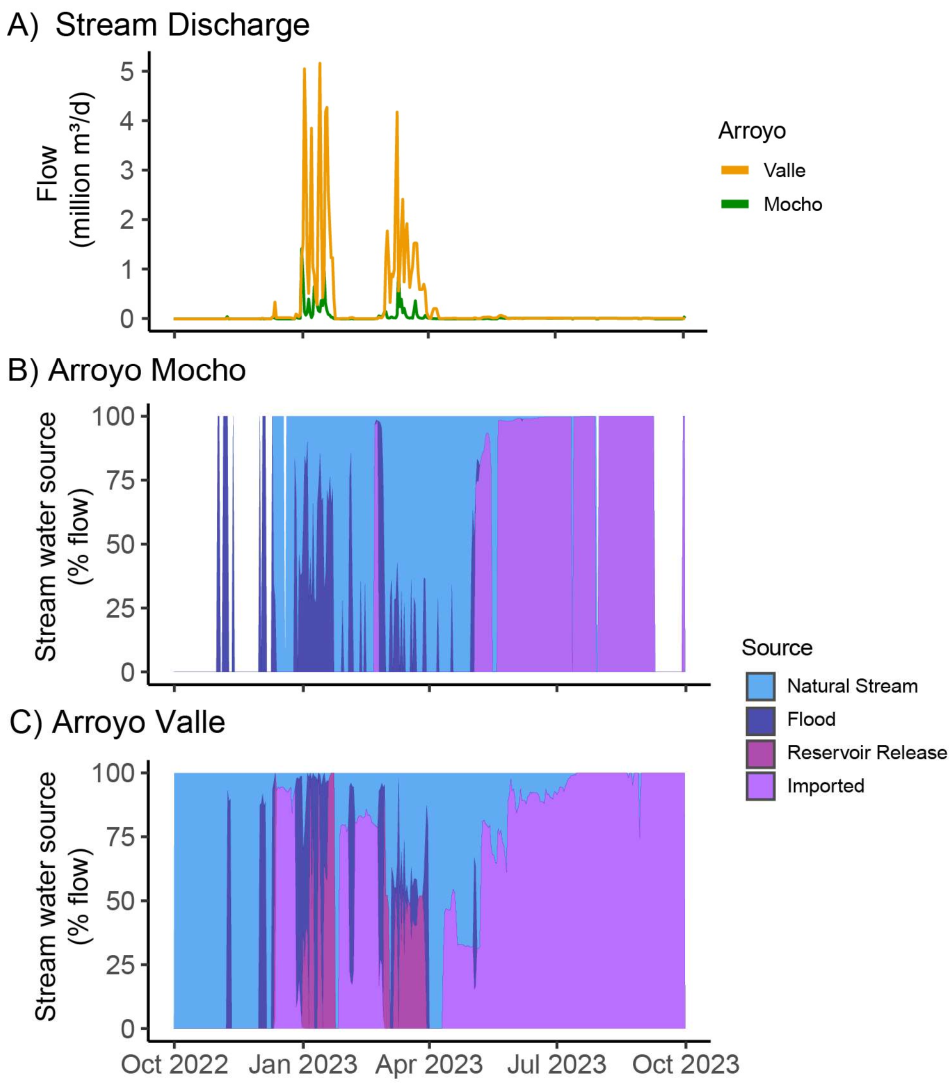

Figure 4. $\delta^{18}O$ values of A) daily precipitation amount, with precipitation-weighted annual mean of $\delta^{18}O$ values. B) $\delta^{18}O$ values of surface waters in the three time periods in WY23, and C) $\delta^{18}O$ values of groundwater samples collected during study period, with dotted lines connecting samples from the same well. The three time periods of water management regimes are marked, allowing us to estimate the average $\delta^{18}O$ values of imported water from the SBA releases. Measurement error is smaller than symbol size.

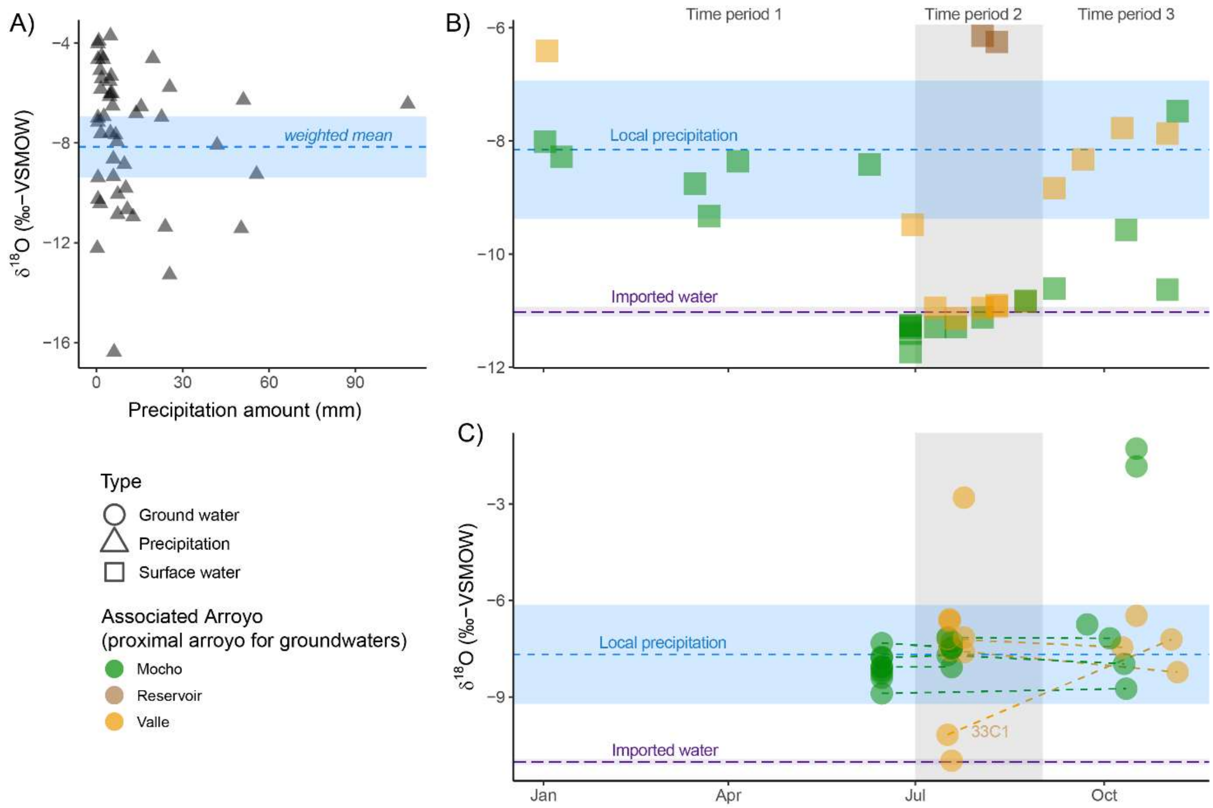

Figure 5. A) ^{35}S activities for precipitation and surface waters, where dashed lines indicate isotope decay curves and B) ^{35}S activities for groundwaters, where colored dashed lines connect samples collected from the same location. Vertical lines at sample points indicate standard error of measurements and open symbols indicate non-detectable ^{35}S activities.

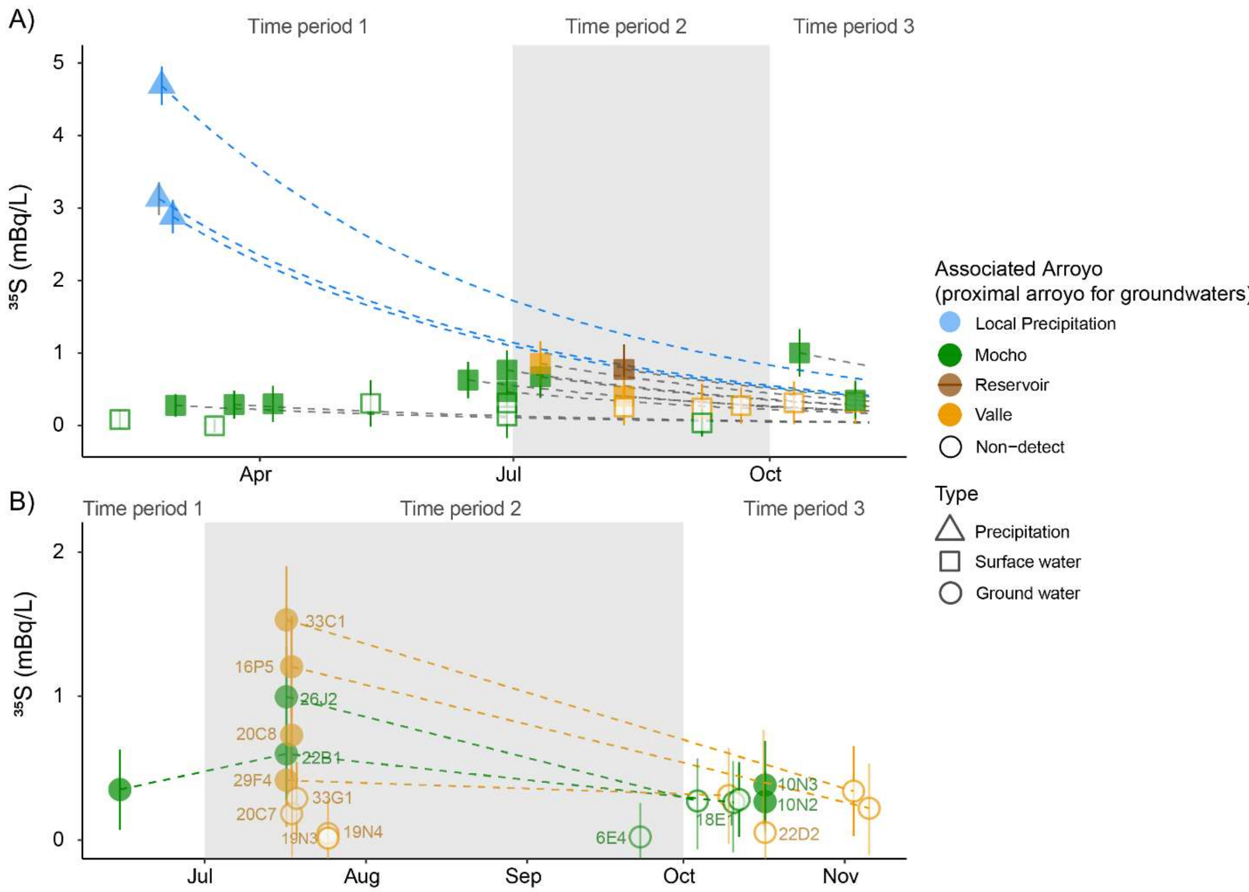

Figure 6. ^{35}S concentrations, decay corrected for A) summer (1 July) and B) fall (1 October) groundwater sampling seasons. The colors indicate water source (based on $\delta^{18}O$) and annotations indicate interpreted age categories (based on ^{3}H).

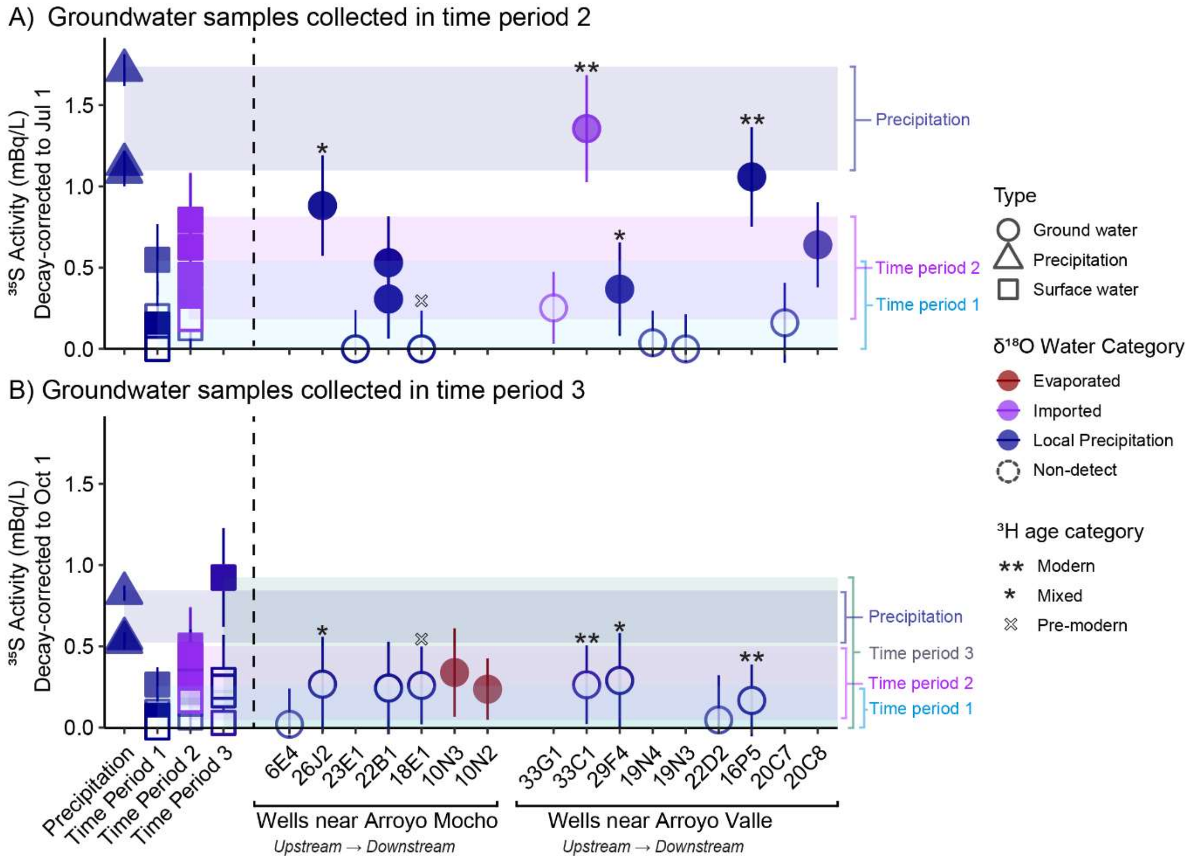

Figure 7. Map of sampled wells (A) with symbols indicating Recharge categories based on both ^{35}S, ^{3}H, and $\delta^{18}O$ data. Locations marked with land use designations. Distance from proximal arroyo (B) and depth of screened interval (C) as a function of recharge categories. Colors indicate proximal arroyo.

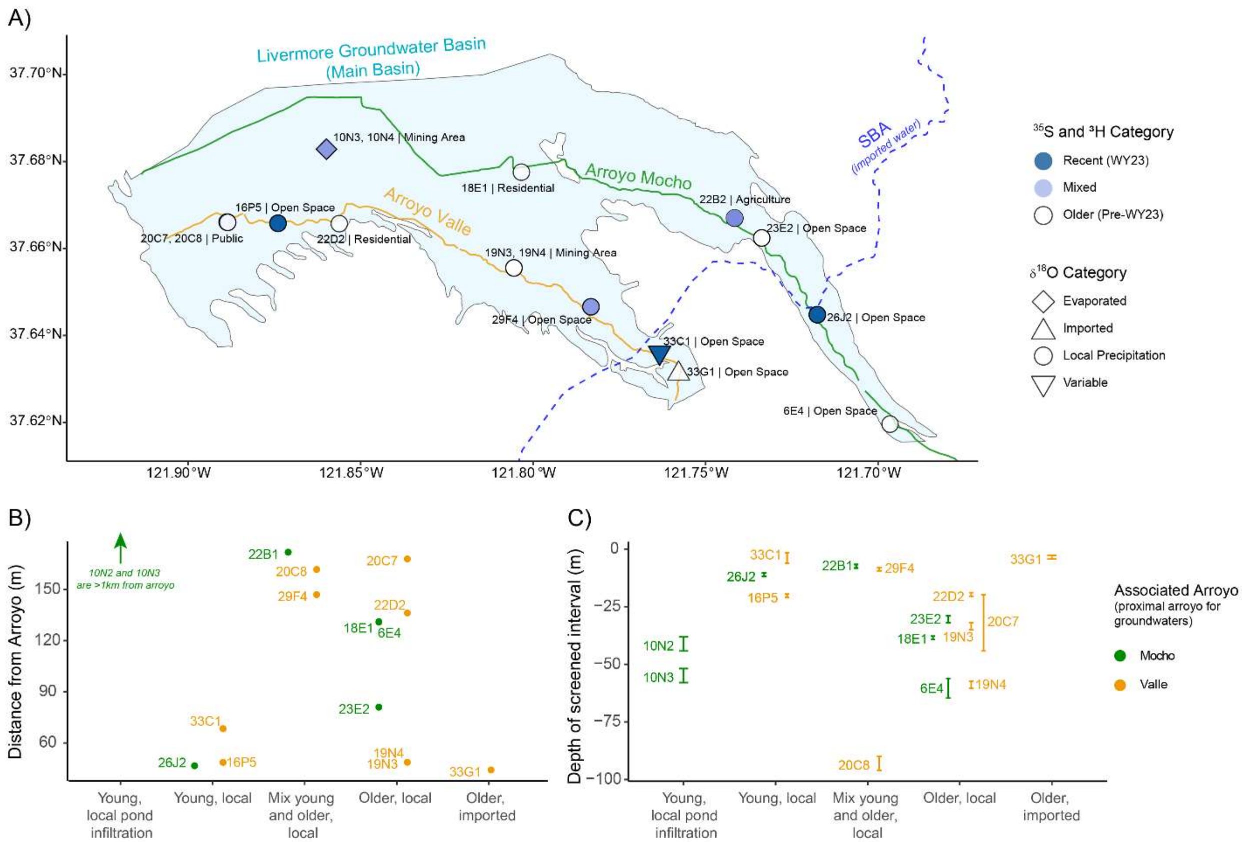

TABLES

Table 1. Isotopic signatures of four potential recharge sources.

Time Period	Sample Type	$\delta^{18}O$ (‰)	^{35}S range of detects, decay-corrected to July 1 (mBq/L)	^{35}S range of detects, decay-corrected to October 1 (mBq/L)	^{35}S detects, non-detects	^{3}H (pCi/L)	Interpretation of Recharge Source
Pre-WY23	Precipitation	HIGH -7.68±3.07	No data	No data	No data	< 9	Older local precipitation
Winter	Precipitation	HIGH -8.16±2.44	HIGH 1.09±0.09 to 1.72±0.10	LOW 0.52±0.04 to 0.83+/-0.05	3, 0	8.2±2.0	WY23 local Precipitation
1 (winter and spring) January – June	Arroyo	HIGH -8.38±0.89	LOW 0.11+/-0.06 to 0.55+/-0.22	LOW 0.05±0.03 to 0.26±0.11	4, 3	8.44±0.78	Natural arroyo streamflow with a small proportion of WY23 precipitation
2 (summer) July – September	Arroyo	LOW -10.87 ±1.05	LOW 0.3±0.2 to 0.8±0.28	LOW 0.22±0.12 to 0.51±0.23	6, 3	8.98±1.05	Imported arroyo streamflow, with a larger proportion of WY23 precipitation
3 (fall) October	Arroyo	HIGH -8.89±1.26	Not applicable	LOW 0.28±0.20 to 0.92±0.30	2, 5	< 8.1±0.6	Mixed imported and local streamflow, containing WY23 precipitation

Table 2. Groundwater isotopic and well description.

Recharge Category	Well Name	δ18O category	^{3}H category	^{35}S category	Top screen depth (m-below ground surface)	Bottom screen depth (m-below ground surface)	Distance from nearest Arroyo (m)
Young, local pond infiltration	10N2	Evaporated		Detect, low	38	44	1321
	10N3	Evaporated		Detect, low	52	58	1321
Young, local precipitation	16P5	Local Precipitation	Modern	Detect, high	20	21	49
	26J2	Local Precipitation	Mixed	Detect, high	10	12	47
Young, variable sources	33C1	Variable	Modern	Detect, high	2	6	68
Mix young and older, local source	20C8	Local Precipitation		Detect, low	90	96	162
	22B1	Local Precipitation		Detect, low	7	8	172
	29F4	Local Precipitation	Mixed	Detect, low	8	9	147
Pre-WY23, local source	1.80E+02	Local Precipitation	Pre-modern	Non-detect	38	39	131
	19N3	Local Precipitation		Non-detect	32	35	49
	19N4	Local Precipitation		Non-detect	57	60	49
	20C7	Local Precipitation		Non-detect	20	44	168
	22D2	Local Precipitation		Non-detect	19	20	136
	2.30E+03	Local Precipitation		Non-detect	29	32	81
	6.00E+04	Local Precipitation		Non-detect	56	65	131
Imported source	33G1	Imported		Non-detect	3	4	44